



ELAXO : Rendering Versatile Resistive Force Feedback for Fingers Grasping and Twisting

Zhong-Yi Zhang

National Chengchi University
Taipei, Taiwan
zychang39@gmail.com

Shih-Hao Wang

National Chengchi University
Taipei, Taiwan
110753102@g.nccu.edu.tw

Hong-Xian Chen

National Chengchi University
Taipei, Taiwan
chenredline@gmail.com

Hsin-Ruey Tsai*

National Chengchi University
Taipei, Taiwan
hsnuhrt@gmail.com

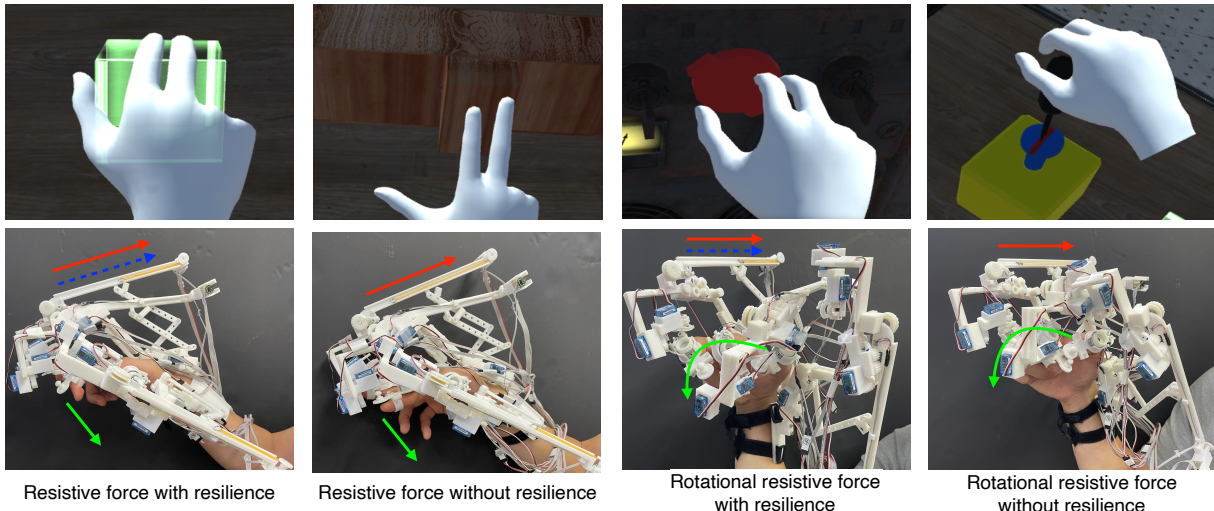


Figure 1: ELAXO renders resistive force and rotational resistive force feedback with resilience or without resilience for grasping/pressing and twisting/turning, respectively. The scenarios for the four conditions are grasping an elastic cube, clamping a tenon and mortise joint, turning a knob with resilience and tightening a screw. The red arrow represents the resistive force, the blue dashed arrow means the resilience and the green arrow is the finger movement.

ABSTRACT

Haptic feedback not only enhances immersion in virtual reality (VR) but also delivers experts' haptic sensation tips in VR training, e.g., properly clamping a tenon and mortise joint or tightening a screw in the assembly of VR factory training, which could even improve the training performance. However, various and complicated manipulation is in different scenarios. Although haptic feedback

of virtual objects' shape, stiffness or resistive force in pressing or grasping is achieved by previous research, rotational resistive force when twisting or turning virtual objects is seldom discussed or explored, especially for a wearable device. Therefore, we propose a wearable device, ELAXO, to integrate continuous resistive force and continuous rotational resistive force with or without resilience in grasping and twisting, respectively. ELAXO is an exoskeleton with rings, mechanical brakes and elastic bands. The brakes achieve shape rendering and switch between with and without resilience modes for the resistive force. The detachable and rotatable rings and elastic bands render continuous resistive force in grasping and twisting. We conducted a just noticeable difference (JND) study to understand users' distinguishability in the four conditions, resistive force and rotational resistive force with and without resilience, separately. A VR study was then performed to verify that the versatile resistive force feedback from ELAXO enhances the VR experiences.

*Corresponding author

Permission to make digital or hard copies of all or part of this work for personal or classroom use is granted without fee provided that copies are not made or distributed for profit or commercial advantage and that copies bear this notice and the full citation on the first page. Copyrights for components of this work owned by others than ACM must be honored. Abstracting with credit is permitted. To copy otherwise, or republish, to post on servers or to redistribute to lists, requires prior specific permission and/or a fee. Request permissions from permissions@acm.org.

UIST '22, October 29–November 2, 2022, Bend, OR, USA

© 2022 Association for Computing Machinery.

ACM ISBN 978-1-4503-9320-1/22/10...\$15.00

<https://doi.org/10.1145/3526113.3545677>

CCS CONCEPTS

- Human-centered computing → Virtual reality; Haptic devices.

KEYWORDS

Haptic feedback, shape rendering, resistive force feedback, wearable device, virtual reality.

ACM Reference Format:

Zhong-Yi Zhang, Hong-Xian Chen, Shih-Hao Wang, and Hsin-Ruey Tsai. 2022. ELAXO : Rendering Versatile Resistive Force Feedback for Fingers Grasping and Twisting. In *The 35th Annual ACM Symposium on User Interface Software and Technology (UIST '22), October 29–November 2, 2022, Bend, OR, USA*. ACM, New York, NY, USA, 14 pages. <https://doi.org/10.1145/3526113.3545677>

1 INTRODUCTION

Haptic feedback has been commonly exploited in virtual reality (VR) interactions. It not only enhances realism in VR games but could even improve performance in VR training by delivering experts' haptic sensation tips, such as when assembling machines in VR factory training or when using a scalpel in VR surgical training. Such VR interactions usually include various and complicated manipulation, *e.g.*, properly clamping a tenon and mortise joint or tightening a screw in assembling, and require haptic devices to provide realistic feedback for more comprehensively delivering the experiences and tips. Although current haptic methods render realistic shape, stiffness and resistive force feedback when pressing or grasping virtual objects, rotational resistive force when twisting or turning virtual objects is seldom discussed. Furthermore, integrating both resistive force and rotational resistive force feedback into a device is essential for versatile VR interactions.

Previous works [6, 8, 11, 15, 24, 39] leverage various braking mechanisms or electrical muscle stimulation (EMS) to limit or move the fingers to render haptic shapes. To further achieve varied degrees of stiffness or resistive forces, current methods [7, 13, 20, 27] exploit motors, propellers or EMS to provide feedback. However, they cannot generate rotational resistive force in twisting or turning. To render rotational resistive force feedback, previous research [14, 16, 19, 26] generates vibrotactile illusions, utilizes propellers or rotates segments of handheld controllers. However, tactile illusions are different from force feedback, and the mechanism on handheld devices cannot be applied to a wearable device. Furthermore, due to the delays or cut-off in the actuation, the methods mentioned prior cannot achieve continuous resistive force. This means that the resistive force cannot continuously change in opposition to the hands' or fingers' movement in these methods, which reduces realism, as proven in [38]. By leveraging the physical properties of an elastic band or spring, continuous resistive force is provided in [28, 38], but only for pressing or grasping instead of twisting and turning. In addition, since the physical properties are used, the continuous resistive force from these methods always accompanies resilience, which limits the VR versatility. For example, resilience is in twisting an elastic cuboid but not in tightening a screw. Therefore, a device rendering shape, continuous resistive force in pressing or grasping and continuous rotational resistive force in twisting or turning is still not achieved, especially for a wearable device.

We propose a wearable device, ELAXO, to render shape, resistive force and rotational resistive force. ELAXO is an exoskeleton on three often-used fingers, including the thumb, index finger and middle finger. For each finger, there are a ring, mechanical brakes and an elastic band. The brakes in the exoskeleton restrict the position of each finger for shape rendering. To further provide resistive force, the rings worn on the fingertips are detached from the exoskeleton after the exoskeleton brakes are locked. When the fingers move, the elastic bands in the exoskeleton are extended to render resistive force. By changing the length and extension distance of the elastic bands, multilevel continuous resistive force feedback is achieved. Since the exoskeleton rotates the rings in different directions before the rings are detached, the rotational resistive force can be achieved via the same elastic bands. A ratchet and pawl design for each elastic band further enables ELAXO to render continuous resistive force with or without resilience. We conducted a just noticeable difference (JND) study to observe users' distinguishability for resistive force and rotational resistive force with and without resilience, a total of four conditions, separately. Based on the results, we further conducted a VR experience study to verify that the feedback from ELAXO enhanced users' experiences, and proposed some applications for ELAXO.

The paper presents the following contributions:

- (1) Proposing a wearable device to render haptic shapes, continuous resistive force and continuous rotational resistive force in grasping and twisting, respectively, with or without resilience.
- (2) Understanding users' distinguishability in resistive force and rotational resistive force with and without resilience, separately.
- (3) Verifying that the versatile feedback from ELAXO enhances users' VR experience.

2 RELATED WORK

We discussed previous works to render haptic shapes, resistive force and rotational resistive force in this section.

2.1 Haptic Shape Rendering

To render shapes, devices changing their shapes into the corresponding virtual shapes is an intuitive but effective approach. Using the pin-based design, inFORM [9] first exploiting 30×30 pins controlled by 900 motors achieves a 2.5D grounded shape display. shapeShift [29], NormalTouch [4] and PoCoPo [44] further apply this design concept in a mobile tabletop device and handheld devices. Elevate [17] utilizes the pin-based design to render shapes for the feet instead of the hands to achieve shape-changing terrains. Furthermore, HapticBots [33] uses mobile robots to accomplish the pin-based design for haptic shape rendering on a tabletop. In addition to the pin-based design, LineFORM [23] and ChainFORM [21] leverage a series of servo motors or servo motor modules to achieve handheld shape-changing devices. Besides, PuPoP [35] uses different shapes of airbags to accomplish a wearable shape-changing device.

On the other hand, devices control fingers' or hands' movements to render haptic shapes. Wolverine [6] and Dexmo [11] exploit mechanical brakes to restrict the fingers from moving inward when

grasping, so the fingers accommodate the virtual shape. Furthermore, their brake designs allow the fingers to freely release the grasped virtual object. DextrES [15] leverages electrostatic brakes to impede the fingers' movements to render shapes when grasping. DextrEMS [24] combines the ratchet and pawl brake design in Dexmo with EMS to render shapes on the fingers. Instead of wearing devices on the fingers, Wireality [8] grounds the device with retractable buckles on the shoulder and connects the wires to the fingers and hand. By braking the retractable wires with solenoids, users feel the shapes. STRIVE [1] further modularizes this design to attach the devices to body parts or objects in the environment for shape rendering. In addition, FingerX [39] leverages extendable and withdrawable extenders on fingers to first achieve shape rendering when the users interact with virtual and real objects simultaneously.

2.2 Resistive Force Feedback

To render resistive force feedback, skin stretch and compression devices [5, 10, 25, 27] are used to render cutaneous illusions of objects' stiffness. Some methods improve the design of shape rendering devices to further render stiffness feedback. inFORCE [22] improves the design of inFORM by exploiting the current sensing to infer the external force and render resistive force feedback of shape and stiffness. Unlike braking mechanism devices only for shape rendering, servo motors can not only control fingers' movements to render shape [30], but also provide stiffness feedback. CLAW [7] combines a servo motor and a force sensor to form a closed loop on a handheld controller and renders resistive force according to the measured force when grasping. PaCaPa [32] leverages two servo motors to push the fingers and hand according to the controller's position, so the user feels stiffness feedback when holding a stick to hit a virtual object. Haptic Links [31] utilizes a servo motor and a mechanical brake on a link to render stiffness feedback between controllers. Thor's Hammer [13] uses six propellers along three axes on a controller to generate resistive force feedback when the user presses virtual objects with different degrees of stiffness. In addition, Virtual Walls [20] exploits EMS to stimulate the user's muscles to render resistive force feedback. However, cutaneous illusions are still different from force feedback. Furthermore, resistive force continuously changes in the opposition to the user's movement. Since these methods exploit discrete actuator control signals or cut-offs to simulate continuous resistive force, the delays from deadband and backlash limit the continuity and realism, as proven in [38].

To render continuous resistive force feedback, Elastic-Arm [2] and FlexiFingers [3] leverage the elasticity of an elastic band and metal stripes between the shoulder and hand, and on the fingers, respectively, for stiffness feedback. Furthermore, [34] restricts the fingerpad deformation to render stiffness/softness feedback on a real rigid object. These methods achieve continuous resistive force feedback but only for one or two force levels. ElasticVR [37, 38] and ElastiLinks [43] control elastic bands' length and extension distance to render multilevel continuous resistive force on the finger, hand and between controllers. CapstanCrunch [28] utilizes capstan drums to magnify the force from a spring controlled by a motor to render human-scale resistive force on a controller when grasping.

HairTouch [18] controls brush hair's length to render stiffness feedback when pressing. These methods generally control the physical properties of objects to accomplish multilevel continuous resistive force feedback. However, these works focus on rendering resistive force in grasping or pressing objects, which means that the force is normal to the fingers or hand. They cannot generate rotational resistive force in twisting or turning. Furthermore, since they use the physical properties of objects, the resistive force always accompanies resilience. Unlike actuator simulation methods, as mentioned prior, able to control the resistive force with or without resilience, these continuous resistive force methods cannot achieve it and limit the versatility.

2.3 Rotational Resistive Force Feedback

To render rotational resistive force feedback, which is usually tangential to the fingers, TORC [19] and PseudoBand [14] utilize force sensors to detect the force exerted by the user and generate vibrotactile illusions on the fingers and between hands when rotating a virtual object. Frictio [12] controls a brake on a ring, so the user can perceive the multilevel rotational resistive force for notification feedback when the other hand rotates the ring. Such a design is also used to render resistive force on the feet for friction feedback in FrictShoes [40]. Furthermore, by modifying and improving the design concept of Thor's Hammer, Aero-plane [16] exploits two propellers on the two sides of a controller to render rotational resistive force on the hand. GamesBond [26] leverages a servo motor to rotate one of two segments connected by a silicone backbone on a handheld controller. By combining two of these controllers on two hands, it renders rotational resistive force on each hand and further generates versatile illusions between hands. However, these methods either render vibrotactile illusions or exploit discrete actuator control to simulate continuous rotational resistive force, which limits the realism, as mentioned prior. Although DragOn [45] adjusts two fans' sizes on a controller and renders continuous resistive force when the user swings or rotates it, the resistive force changes according to the fans' size and speed of the hand movement, which is different from the resistive force changing in the opposition to the user's movement. Furthermore, these rotational force feedback designs either require two hands in the interactions or are for a handheld controller. Rotational resistive force feedback for fingers on wearable devices or exoskeletons is still not explored.

3 ELAXO

To render versatile resistive force feedback in various scenarios or complicated manipulation to enhance immersion and deliver experts' haptic sensation tips in VR training, we designed and built the ELAXO prototype.

3.1 Design Considerations

We took the following design considerations into account for ELAXO.

- *Realism.* Rendering realistic resistive force feedback is essential. Based on the ElasticVR [38], resistive force continuously changes in opposition to the users' movement. In resistive force simulation, the delays from deadband and

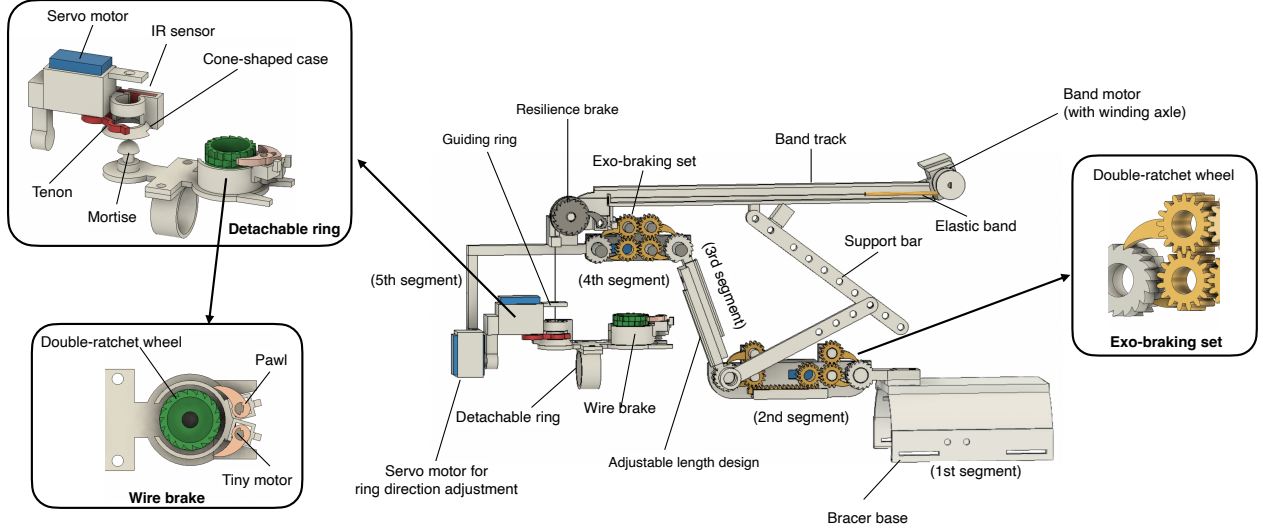


Figure 2: The 3D model of the EXALO prototype with only one finger for illustration.

backlash in discrete actuator control limit the realism. Therefore, leveraging and even controlling objects' physical properties, e.g., elastic bands, springs or metal strips [2, 3, 28, 38], is adopted in our design to render continuous resistive force and achieve realism.

- **Versatility.** Since our goal is to render versatile force feedback in various VR scenarios or training, versatility is critical to determine the number of types of interactions or manipulation that our system can render. If the number is low and using a substitute resistive force type for simulation, it could even affect the realism. For continuous resistive force methods based on the realism design consideration, multilevel continuous resistive force is achieved by previous works [28, 38]. However, neither rendering rotational resistive force when twisting or turning virtual objects nor generating continuous resistive force without resilience is accomplished. Thus, we integrate all these properties into our design, and the combinations of these properties increase the versatility.
- **Dexterity.** Dexterity is an important issue for wearable devices. For exoskeletons across several body joints, insufficient degrees of freedom could make the users feel restricted or even uncomfortable. Therefore, high degrees of freedom are used in our design to maintain dexterity.

3.2 Hardware Implementation

ELAXO is an exoskeleton worn on three often-used fingers, including the thumb, index finger and middle finger. The other end of the exoskeleton is worn and grounded on the wrist. For each finger, there are a ring, mechanical breaks and an elastic band in the exoskeleton. The exoskeleton with brakes renders haptic shapes. Each detachable and rotatable ring in the exoskeleton is connected to an elastic band to render continuous resistive force and continuous rotational resistive force after the exoskeleton brakes are locked.

A resilience brake between the ring and band is used to achieve continuous resistive force with or without resilience.

For the exoskeleton for each finger (Figure 2), we were inspired by the braking mechanisms in [11, 24]. They exploited a ratchet as well as a pawl or a stopping slider to control a brake on a finger joint. When a pawl disengages a ratchet, there is no resistive force or restriction for the free movement. When the pawl engages the ratchet, only low power or even no power is required for the self-locking brake to provide a strong force for braking or locking in one direction. Thus, to render shapes, the brake prevents the finger from moving inward so the finger accommodates the virtual object's shape during grasping, but it allows the finger to freely move outward. Although such a one-direction brake enables users to perceive the shape of a rigid virtual object and freely release it, we require a two-direction brake to fix the exoskeleton firmly when attaching and detaching the ring to further render resistive force. Therefore, we 3D printed a double-ratchet wheel by combining two opposite ratchets into two adjacent layers. By driving one of the two opposite pawls on the two connected gears in two layers, the double-ratchet wheel on a finger joint could be unlocked or locked in both directions, which only requires low power. Furthermore, by modifying the design in [11], a servo motor (XCSOURCE RC450) can control four pawls of two double-ratchet wheels on two joints via gears or a rack and pinion design, which is an exo-braking set.

To maintain dexterity and higher degrees of freedom of each finger, four double-ratchet wheels from two exo-braking sets are on the four joints, including the wrist, metacarpophalangeal (MCP), proximal interphalangeal (PIP) and distal interphalangeal (DIP) joints. Therefore, these four joints connect five segments achieve a four degrees-of-freedom (4DoF) exoskeleton for each finger. The first segment is a 3D-printed bracer worn on the wrist via two Velcro straps. Silicone pads are attached to the inside of the bracer to increase friction and stability between the bracer and wrist. These silicone pads also enhance the comfort when wearing the rigid

bracer and can adjust the bracer for varied wrist sizes. The second segments of all fingers are grounded on the same first segment as a base. The second and fourth segments are actually two exo-braking sets, respectively. The third segment with an adjustable length design using two screws and nuts allows the exoskeleton to be fit for different hand sizes. The fifth segment is connected to the ring worn on the fingertip. In fact, we had tried to ground the exoskeleton on the back of the hand instead of the wrist, which could reduce the exoskeleton size and the number of segments. However, when twisting or turning, the relative movements between the fingers and the hand are too small, which reduces the effect of rotational resistive force rendering. Therefore, the current five-segment design renders better performance. Since the DIP and PIP joints are 1DoF joints, and the MCP joint and wrist are 2DoF joints in anatomy, the dexterity of DIP and PIP joints is maintained, and the 1DoF, which is the major one, in the MCP joint and wrist is also provided. The missing 1DoF in the MCP joint and wrist in the exoskeleton is restricted in order to render rotational resistive force. Otherwise, the horizontal DoF counteracts the rotation resistive force. The major restriction is in the MCP joint of the dexterous thumb. Although we could add a braking set for this DoF, it increases the size and weight of the device. Therefore, such a design still achieves high degrees of freedom for the fingers to freely move without restrictions, which accomplishes the versatility and dexterity design considerations.

A ring is connected to an elastic band (band length: 54mm) via a fishing line. An elastic band is placed in a band track, which is combined with the fifth segment of each finger. Although such a design could increase the burden on the finger, it allows the fishing line to be directly connected between the band and the ring without generating additional resistive force between the line and exoskeleton. The other side of the elastic band is connected to a winding axle via a fishing line (radius: 3.5mm) on a DC motor (Pololu Micro Metal Gearmotor with gear ratio 380:1) with a rotary encoder (Pololu Magnetic Encoder 12 counts per revolution) on the end of the track. The motor winds the elastic band to adjust the band's length in the track to change its elasticity since only the part of the band in the track could be extended. Therefore, different levels of continuous resistive force are rendered. The concept of changing the length and extension distance of an elastic band to render multilevel continuous resistive force is based on [38, 43], which achieves the realism design consideration. Besides, to reduce the weight of the track and motor on the finger, a joint with two support bars is between the track and the second segment on the hand.

Furthermore, when the elastic band is extended by the finger, the user can not only perceive the resistive force when moving the finger when grasping or twisting but also feel the resilience force even if stopping moving the finger. Since continuous resistive force always accompanies resilience, we leveraged a ratchet and pawl design to build a one-direction resilience brake to switch between with and without resilience modes. Therefore, a ratchet and a pawl are placed on the other end of the track. The 3D-printed ratchet is combined with a pulley with a bearing in two adjacent layers. It is between the elastic band and the ring, so the fishing line between them is located in the groove of the pulley with one loop. A rubber band is affixed to the groove to increase the friction between the groove and the fishing line. While the pawl disengages the ratchet,

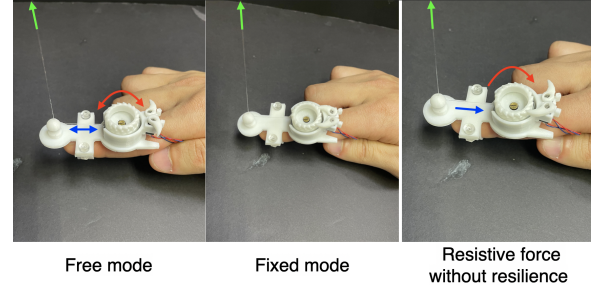


Figure 3: The three modes of a wire brake.

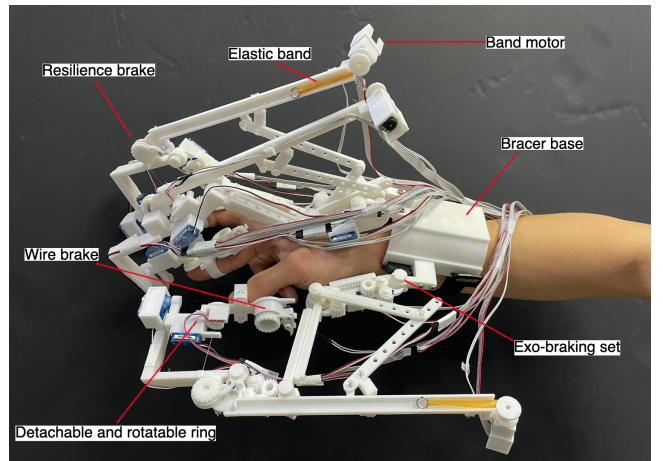


Figure 4: The ELAXO prototype worn on the three fingers.

the ratchet with the pulley rotates accordingly when the elastic band is extended via the fishing line, so the users can perceive resistive force with resilience. When the pawl, which is controlled by a tiny motor (Pololu Vibration Motor 11.6×4.6×4.8mm), engages the ratchet, the one-direction resilience brake prevents the resilience from being delivered to the finger. However, it still allows the resistive force to be delivered to the finger if the band is further extended. Furthermore, the ratchet with the pulley is also a fixed pulley, so it can change the direction of the fishing line from along the track to toward the ring beneath it, which is about 90°. Therefore, the resilience brake enables ELAXO to render two resilience modes for the versatility design consideration.

To achieve a detachable and rotatable ring connected to the exoskeleton, a cone-shaped case and a ring with a small cylinder above it are used for detachment. A servo motor controls a tenon besides the case. A mortise is around the cylinder and a bullet head shape is on top of it. The cone-shaped case and the bullet head shape make the ring easily move back into the case, and the mortise around the cylinder allows the tenon to easily clamp with it. An infrared (IR) sensor (QTR-1RC Reflectance Sensor) on the case is used to detect whether the ring's mortise is in the case or not. The motor then rotates the tenon to clamp or release the mortise to attach or detach the ring. The case is connected to the shaft of another servo motor. This servo motor is in the fifth segment to adjust the direction to detach the ring. Furthermore, a guiding ring

above the cone-shaped case is used as a fixed pulley, so the fishing line from the elastic band passes through the guiding ring, cone-shaped case and small hole on the cylinder, then connected to the ring. Therefore, when the servo motor rotates the case to adjust the ring direction, the guiding ring is rotated accordingly and changes and guides the direction of the fishing line smoothly. Such a design switches between modes for rendering continuous resistive force or continuous rotational resistive force using the same elastic band. In addition, the center of the ring is along the shaft of the servo motor, so during the adjustment, the ring is rotated by the servo motor but does not move the finger. Furthermore, the friction is low between the 3D-printed PLA ring and the finger, so the finger is not twisted by the ring during the adjustment. These servo motors are the same type as those in the exo-braking sets.

In addition, there are three modes for the fishing line between the elastic band and the ring. During the ring direction and band length adjustments, the distance between the band and the ring is varied. The length of the fishing line should be automatically adjustable to pull the band taut but not extend it. Such a free mode does not generate resistive force from the band but is able to extend the band immediately when the ring is detached. For the resistive force delivery, the fishing line must be tight with a fixed length. In such a fixed mode, the band can completely deliver the resistive force and resilience to the ring. For rendering resistive force without resilience, the length of the fishing line should be fixed when grasping or twisting to extend the band. However, when moving the finger back to grasp and twist again, the fishing line should be shortened to maintain it taut since the resilience brake prevents the band from contracting, which makes the resistive force being delivered instantly and smoothly for next the grasping or twisting. Therefore, by modifying and improving the designs in [1, 8, 38], we exploited a retractable buckle with a wire brake to switch among these three modes, as shown in Figure 3. We modified the retractable buckle by replacing its cotton line with the fishing line connected to the band to reduce the friction of the line. We further attached another double-ratchet wheel, as mentioned in the exo-braking sets, to its winding axle. Unlike in the exo-braking sets, two tiny motors, the same type as that in the resilience brake, need to independently control two pawls to switch three modes. When the two pawls disengage the double-ratchet wheel, the brake is unlocked for the free mode. While the two pawls both engage it, the brake is locked for the fixed mode. When only one pawl engages it, the wire brake becomes a one-direction brake. Therefore, the fishing line cannot be pulled out from the retractable buckle but can be retracted, which achieves the requirement for rendering resistive force without resilience.

We fabricated rings of different sizes for various fingers and users. They are switchable using screws and nuts. There are four servo motors, four tiny motors, a DC motor and an IR sensor on the exoskeleton for each finger. Therefore, a total of twelve servo motors, twelves tiny motors, three DC motors and three IR sensors are on ELAXO. The servo motor and tiny motors require a 6V power supply, and the DC motors need a 12V power supply. The twelves tiny motors and three DC motors are connected to eight motor drivers (Dual TB6612FNG). The motor drivers, servo motors and IR sensors are connected to an Arduino Mega board. The six signal wires from the encoders of the three DC motors are connected to

the board. The weight of ELAXO is about 540g, and the workspace of the exoskeleton is approximately 4726 to 6076 cm³ depending on the fingers' pose. The ELAXO prototype is shown in Figure 4.

3.3 Software Control Flow

To render continuous resistive force and continuous rotational resistive force with or without resilience, 4 modes (= 2 (resistive force directions) × 2 (resilience modes)) are switched in ELAXO. To further include the free movement mode and shape rendering mode, there are a total of 6 modes rendered by ELAXO. The software control flow of ELAXO is illustrated in Figure 5.

Initially, the device is in the free movement mode, which means the hand and fingers can freely move without any resistive force or restriction. All rings are attached to the exoskeleton and all brakes are unlocked. During grasping a virtual object, when the fingers contact the virtual object, the exo-braking sets are locked correspondingly with the delay of 30ms. Therefore, the fingers accommodate the virtual object's shape in the shape rendering mode. When the hand contacts the virtual object, the system delivers its properties to the device, including its resistive force magnitude of level, it can be grasped or twisted and its resistive force with or without resilience. Therefore, after the exo-braking sets of the finger first contacting the virtual object are locked, for each finger, the band motor adjusts the elastic band's length for proper force level, the direction servo motor adjusts the ring direction if the object can be twisted, and the resilience brake is locked if the resistive force is rendered without resilience. The ring direction and resilience brake adjustments are performed in the same time after the resistive force adjustment, which prevents the adjustments from being interfered with, but the adjustments on different fingers could be performed simultaneously. After all exo-braking sets are locked and all adjustments in all fingers are done, the wire brakes are locked in one of the two modes based on the resistive force with or without resilience, and then all rings are detached from the exoskeleton.

Notably, the default ring direction is vertical downward. Therefore, after perceiving the object's shape, the user could further grasp or press it in the normal direction to feel its stiffness due to the extended elastic bands. For twisting or turning a round virtual object, the ring direction should be adjusted to 90° to the default direction so the fingers' movements are tangential to the object and perceive the rotational resistive force. However, twisting objects with different shapes causes varied finger movement directions, and 90° to the default direction could make the rings easily collide with the exoskeleton's fifth segments of the adjacent fingers. Therefore, we set the ring directions to 45°, 60° and 60° to the default direction for the thumb, index finger and middle finger, respectively, which prevents the collision issue. The ring direction adjustment changes the direction of two key mechanisms, cone-shaped cases and guiding rings, as mentioned above. The cone-shaped cases guide the ring detachment directions, so the user has to rotate the fingers in the corresponding directions to detach the rings and perceive rotational resistive force. The guiding rings as fixed pulleys guarantee that the rings move smoothly in rotational resistive force feedback. These two mechanisms effectively guide the user to perform the twisting or turning gestures, so the user can perceive rotational

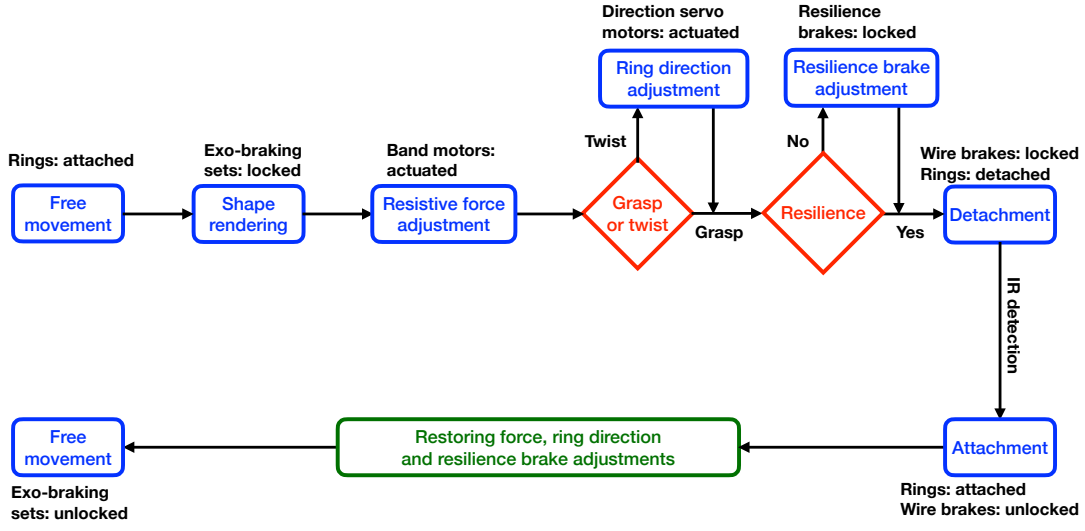


Figure 5: The software control flow of ELAXO.

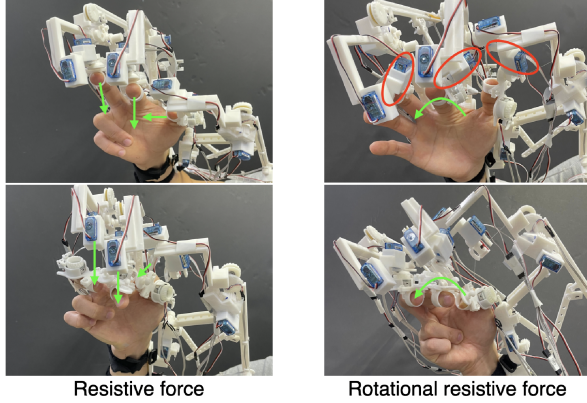


Figure 6: The user grasps after the rings are detached to perceive resistive force (left). The rings directions are adjusted (in the red ellipses) before being detached, so the user twists to feel rotational resistive force (right).

resistive force feedback, as proven in the VR study. In addition, our design in ELAXO could only adjust the ring to one direction for twisting or turning. Since users usually rotate the hand outward or supination to perceive gradually-increased rotational resistive force when twisting or turning in daily lives, e.g., turning a knob or tightening a screw, this is set as the default direction for twisting. Certainly, the twisting direction of virtual objects could be set to either hand outward (supination) or inward (pronation) rotation, but could be both of them. This is a limitation of the current design.

After detaching the rings, the user can freely grasp or twist the virtual object and perceive continuous resistive force or continuous rotational resistive force (Figure 6), respectively, and the IR sensors detect whether the rings move back to their cone-shaped cases on

the exoskeleton. Since the user perceives the force from the elastic bands and retractable wires pulling the fingers, the user can follow the force to move the rings back and attach them to the exoskeleton, which reduces misalignment as proven in the VR study. When the rings are attached to the exoskeleton, the wire brakes are unlocked, and the adjustments are restored simultaneously. Notably, the band motors release the elastic bands a bit loosely beyond their initial states to make the resilience brakes easily be unlocked, and then move the bands back to the initial positions. After all adjustments in all fingers are restored, the exo-braking sets are unlocked. Therefore, ELAXO is back to the free movement mode again and the user can release the virtual object.

3.4 Resistive Force Measurement

To understand the properties of the rendered resistive force, we performed a hardware evaluation for resistive force measurement to obtain the relationships between the elastic bands' extension distance and elastic force in different bands' lengths. We built an aluminum extrusion frame and affixed a force sensor (TAL220 with an HX711 amplifier) to it. Furthermore, we fabricated a band track connected to a fifth segment with a base, the same as in the exoskeleton, so it could be attached to the frame. As mentioned prior, a ratchet with a pulley on the end of the band track is used to change the direction of the fishing line from the elastic band to the ring, about 90°. The fishing line further passes through the guiding ring, cone-shaped case, and small hole on the cylinder above the ring, and it is connected to the modified retractable buckle controlled by the wire brake on the ring. These designs were all included in the device with the base we built, so we could measure the resistive force perceived by the finger in real conditions, including the resistive force from the fishing line passing through these parts. Furthermore, as in the band length adjustment in real conditions,

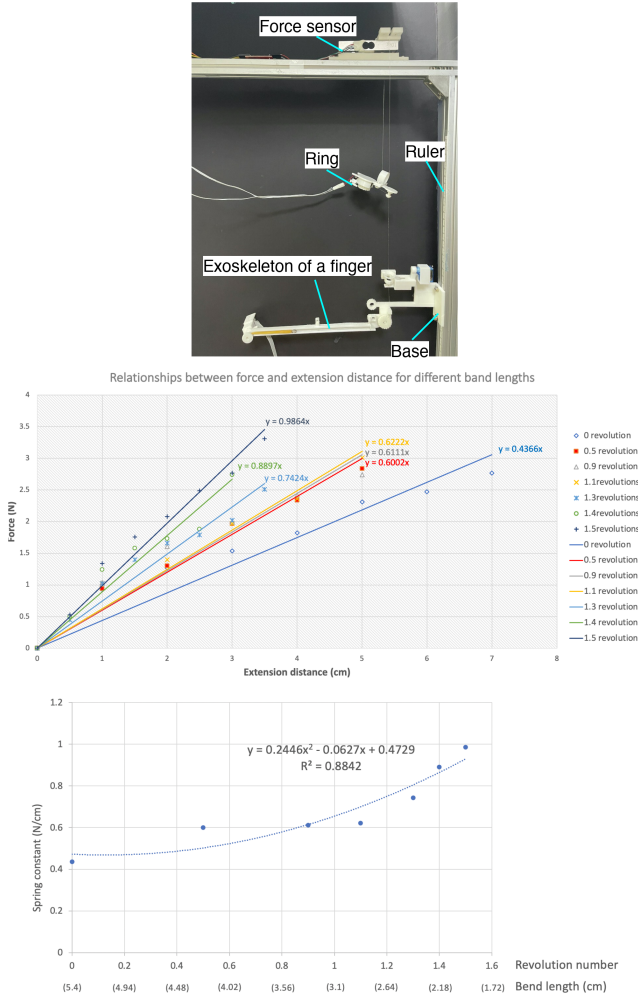


Figure 7: The setup to measure the force (upper). The band's length is controlled by the revolution number of the band motor. The relationship between the band's length (revolution number) and spring constant (middle). The relationships between the elastic force and extension distance of an elastic band with different band lengths (lower).

the retractable force from the retractable buckle pulled the other side of the elastic band when adjusting the length of the elastic band by rotating the band motor in the device with the base on the aluminum extrusion frame.

Since we intended to measure the resistive force perceived by the users without the weight of the ring and wire brake, the force sensor, ring and the base were placed vertically, as shown in Figure 7 (upper). We measured the weight of the ring in advance, and then hung the ring on the force sensor via a fishing line, so the weight and the resistive force were both measured by the force sensor. Therefore, by subtracting the weight from the measured force data, the resistive force without the weight of the ring and wire brake was obtained. Furthermore, a ruler was attached to the side of the aluminum extrusion bar beneath the base. We moved the base to

a position that made the elastic band taut but not being extended as the initial position, which means that the force sensor should still only measure the weight of the ring and the wire brake. By moving and affixing the base to different positions, the force sensor recorded the resistive force and the extension distance was the distance between the current and the initial positions of the base using the ruler.

By repeatedly measuring five different extension distances for each one of the seven lengths of the band, between 0 and 1.5 band motor revolutions from a pilot study, we obtained the relationships between the resistive force and extension distance of these seven lengths of the band. By computing a linear regression line passing through the origin for each band length, its slope is like a spring constant k in Hooke's law ($F = -kx$), as shown in Figure 7 (middle). Although elastic bands do not completely follow Hooke's law like springs, the results are quite consistent with Hooke's law. Therefore, we leverage these spring constants to represent the properties of the resistive force in different lengths of the band in this paper herein. Furthermore, by computing the quadratic regression curve to obtain the relationship between the band's length and spring constant, we could further understand how to render other spring constants by controlling the band motor revolution number to adjust the band's length (Figure 7 (lower)).

4 JUST NOTICEABLE DIFFERENCE STUDY

We conducted a just noticeable difference (JND) study to understand users' distinguishability of resistive force and rotational resistive force with and without resilience, a total of four conditions, separately. Although the JND study of the continuous resistive force in hand pressing had been performed by ElasticVR [38], its JND results of the hand cloud not be applied to the fingers due to different distinguishability in varied body parts. Furthermore, we also focused on observing whether users' distinguishability of resistive force and rotational resistive force were different, and whether resistive force with or without resilience affected the distinguishability in this study.

4.1 Participants and Apparatus

The ELAXO device was worn on the participants' dominant hand. They wore a Vive Pro head-mounted display (HMD) on the head and held a controller with the other hand. The HMD isolated the participants' visual feedback from the device and showed the items for selection, the controller was used to select the answers to the trials. The earphones of the HMD played white noise to prevent the noise of the motors, as in [36, 42]. 12 participants (2 female, all right-handed) aged 22–28 (mean: 23.83) were recruited. The mean hand length and width were 17.93cm and 9.92cm, respectively.

4.2 Task and Procedure

A one-up, two-down staircase design [41, 42] was adopted in this JND study. Unlike conventional JND stimuli with certain intensities, e.g., a certain temperature, vibration frequency or force magnitude, applying to or stimulating the participants, the resistive force magnitude in the stimuli of this study continuously changes when moving the fingers. Therefore, instead of a certain force magnitude, we chose a spring constant, k , for each continuous resistive force

stimulus in our JND study, as mentioned prior, and the participants had to actively move their fingers to acquire and perceive their stimuli. There were three stimuli in a trial, including two reference stimuli (S) and a test stimulus ($S + \Delta S$). The spring constant of S was 0.44 N/cm, which was the lower bound of the spring constant range from ELAXO, and ΔS was an adaptively determined positive number as the spring constant difference between the reference and test stimuli. The initial step size of ΔS was 0.22 N/cm (50% of S). If the participants responded correctly two consecutive times or incorrectly once, ΔS was respectively decreased or increased by 0.044 N/cm (10% of S). After the first reversal, which means a change from decreasing to increasing ΔS and vice versa, ΔS was decreased or increased by 0.022 N/cm (5% of S), after consecutive two correct answers or one incorrect response, respectively. Furthermore, if ΔS was 0 or the test stimulus exceeded 0.98 N/cm, the system considered it as a reversal. A staircase run ended after five total reversals, and the average from the last four reversals was calculated as the threshold.

The participants sat on a chair and the elbow could lay on the armrest or a desk to reduce fatigue, but the arm and wrist should be in the air to guarantee sufficient space for moving and perceiving. The experimenter introduced the device and study procedure, chose the proper rings, and wore and calibrated the device on the participants. The time of wearing the device with the experimenter's assistance is about 40 sec. The average setup time, including the time of the third segment adjustment, the support bars adjustment, and ring choosing for each finger, is approximately 200 sec. In the beginning, the participants were asked to open their hand, the exo-braking sets were locked and they then grasped or twisted to perceive the resistive force stimulus. After perceiving, they moved back the fingers to attach the ring to the exoskeleton and pressed the touchpad on the controller with the non-dominant hand. The band motors released all bands and wound them to render the next resistive force stimulus. After perceiving the three stimuli, three items were displayed on the HMD, they selected the one with the resistive force different from the others, the test stimulus, using the controller. They could also play back the stimuli to perceive again if they were not sure about the answer. The order of three stimuli in each trial was randomized. Four staircases were performed for the 4 conditions (= 2 (resistive force directions) \times 2 (resilience modes)), respectively. The order of two resilience modes in resistive force and rotational resistive force was counterbalanced, and the order of two resistive force directions was also counterbalanced. They could have a break between sessions to prevent the fatigue from affecting the distinguishability. We interviewed them after the experiment. The study, including the introduction and interview, took about two hours.

4.3 Results and Discussion

The JND results are shown in Figure 8. Repeated measures ANOVA and Bonferroni correction for post-hoc pairwise tests were adopted for the analyses. No significant main effect is found the resistive force direction ($F_{1,11} = 4.27, p = 0.06$), but a significant main effect ($F_{1,11} = 33.741, p < 0.001$) is revealed in the resilience mode. There is no significant interaction effect ($F_{1,11} = 0.32, p = 0.58$) between the resistive force direction and resilience mode. To further analyze

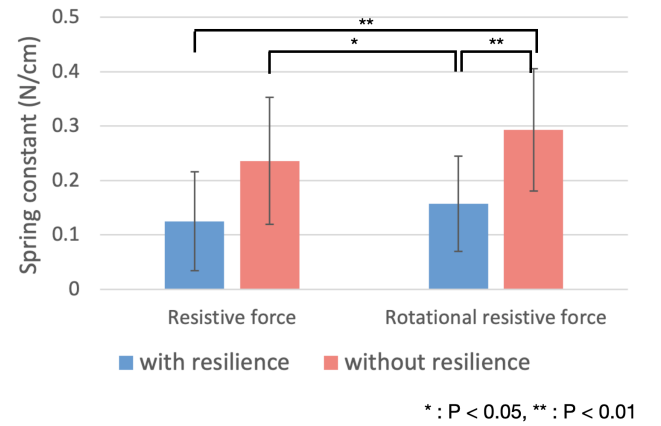


Figure 8: The results of the JND study in the four conditions.

the results of the four conditions, the post-hoc pairwise tests show that no statistical significance is between with (0.125 N/cm, JND = 28.41%) and without (0.236 N/cm, JND = 53.64%) resilience modes in resistive force ($p = 0.06$), but significant difference is between with (0.157 N/cm, JND = 35.68%) and without (0.293 N/cm, JND = 66.59%) resilience modes in rotational resistive force ($p = 0.001$). Furthermore, there is no statistical significance between resistive force and rotational resistive force with or without resilience. Therefore, the results show that the users have similar distinguishability of resistive force and rotational resistive force. However, the distinguishability for the force with resilience is better than that without resilience.

Most participants except for *P1* agreed that the stimuli of the resistive force were more distinguishable than the stimuli of the rotational resistive force. They supposed that the movements to perceive resistive force were more conventional and intuitive than those for rotational resistive force. Although *P1* thought that twisting or turning movements could extend the bands longer to easily perceive the force, *P4, P6, P8* and *P12* commonly mentioned that the muscles and joints to perform these movements were more complicated and less used. Furthermore, *P3, P7* and *P11* said that the rings sometimes collided with the exoskeleton of the adjacent fingers or their own cone-shaped cases when twisting, which interfered with distinguishing. On the other hand, most participants except for *P4* supposed that the stimuli with resilience were more discriminative than those without resilience. They commonly believed that resilience was also a cue or reference force to differentiate among the stimuli, so lack of the cue in the conditions without resilience reduced the distinguishability. In addition, *P5, P7, P8* and *P12* suggested that the force increased from and then decreased back to zero whenever they grasped or twisted in the stimuli with resilience, but the force kept increasing in the stimuli without resilience, which increased the difficulty of differentiating. Although *P4* could clearly perceive the difference between with and without resilience modes, s/he did not think that the factor affected the distinguishability.

The comments are quite consistent with the statistical results. Although there is no significant effect, resistive force is more distinguishable than rotational resistive force based on the comments and

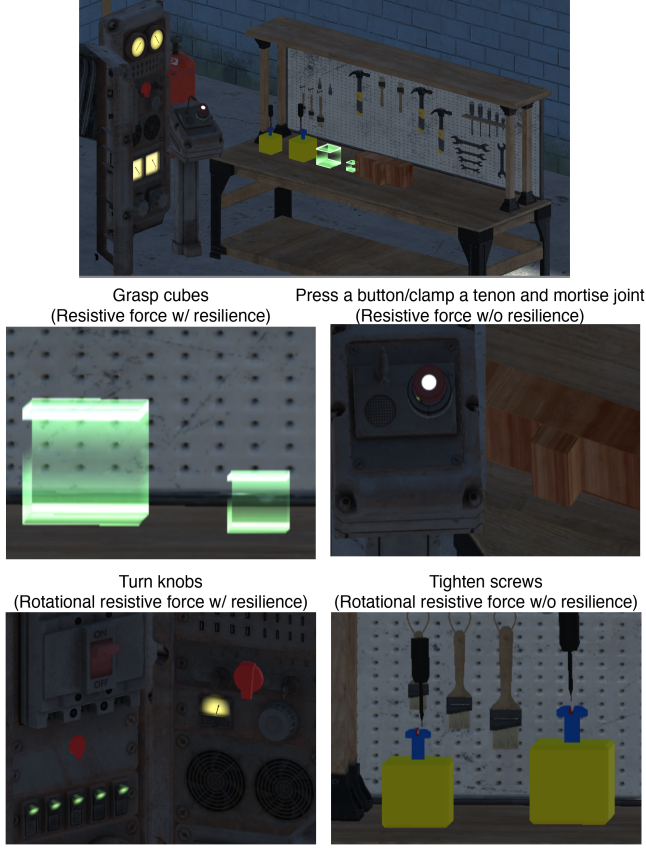


Figure 9: The virtual factory scene of the VR study. 8 tasks of the 4 conditions are in the scene.

the average thresholds. A marginally significant effect ($p = 0.06$) is in the resistive force direction factor. The stimuli with resilience are significantly more distinguishable than those without resilience. The results show that the change of the spring constant is at least 66.59% higher than the current spring constant for users to clearly distinguish the difference in all four conditions.

5 VR EXPERIENCE STUDY

We conducted a VR experience study to observe that compared with current methods, whether the versatile resistive force feedback from ELAXO enhanced users' VR experiences.

5.1 Participants and Apparatus

The study setup was basically the same as in the JND study. To track the hand's and fingers' movements for grasping and twisting, a Vive tracker was attached to the side of the base of ELAXO and a bending sensor was attached to each finger (Figure 10). 12 participants (3 female, all right-handed) aged 23–25 (mean: 24.17) were recruited. None of them had attended the previous study. The mean hand length and width were 18cm and 9.54cm, respectively.

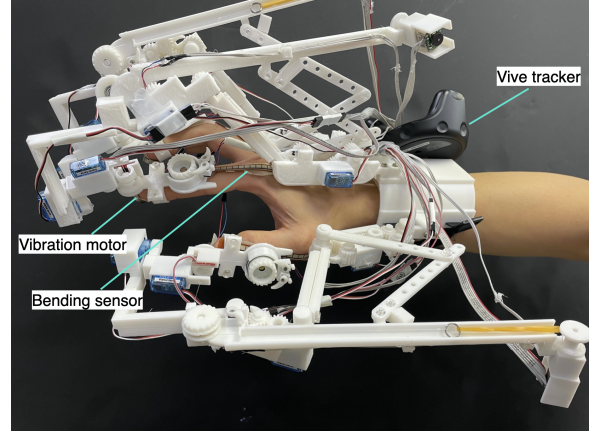


Figure 10: The setup of the VR study. Bending sensors and a Vive tracker were used to track the fingers and the hand. Vibration motors were attached to the fingertips in the vibrotactile feedback method.

5.2 Task and Procedure

We built a scene of a VR factory, as shown in Figure 9. A total of 8 tasks from the 4 conditions with the 2 force levels for each condition were designed. Based on the JND results, we chose two force levels with the spring constants 0.44 N/cm and 0.74N/cm, which made the spring constant at level 2 68.18% higher than that at level 1. The delays of level 1 (without resistive force adjustment) and level 2 (with 1.3 band motor revolutions) are 60ms and 2460 ms, respectively. Notably, the delays are before instead of during grasping or twisting to perceive force feedback. For resistive force with resilience, the participants grasped two cubes with different sizes and degrees of stiffness or elasticity. For resistive force without resilience, they pressed a button on a machine to perceive the force at level 1, and pressed to clamp a tenon and mortise joint on a desk and feel the force at level 2. For rotational resistive force with resilience, they turned two knobs on a machine of different sizes to perceive the feedback at the two force levels. For rotational resistive force without resilience, they tightened two screws of different sizes using two screwdrivers to feel the feedback at the two force levels. Most of the tasks were common scenarios in the virtual factory or assembly training. All these machines and objects were placed around the participants. This shows the benefits of our wearable device, which allows the users to freely move in VR to explore and perform various tasks.

Three feedback methods were compared in this study, including vibrotactile feedback (V), resistive force (R) and ELAXO (E). In all methods, the participants wore the ELAXO device to perceive shape feedback as in common exoskeletons. For (V), three coin vibration motors were attached to the fingertips, and the ELAXO device only rendered haptic shapes but the rings were not detached, so it did not provide resistive force. When the participants grasped or twisted virtual objects, the vibration motors generated vibrotactile illusions with different intensity changes to simulate multilevel resistive force feedback (Figure 10). This was a common approach for the exoskeletons rendering only shape but not stiffness feedback,

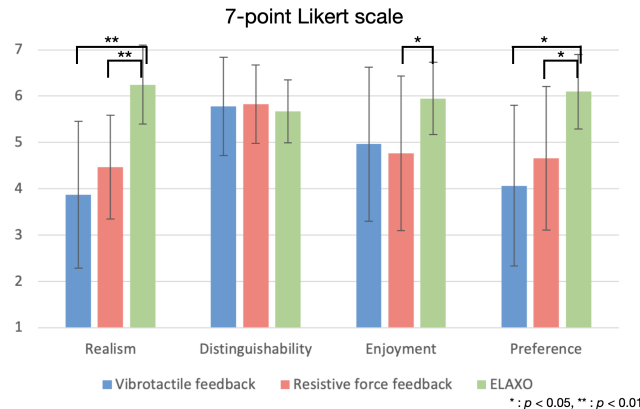


Figure 11: The results of the VR experience study on a 7-point Likert scale.

which was used as a baseline in the comparison. For (R), the ELAXO device only rendered multilevel resistive force with resilience for all tasks, which means that the ring direction adjustment and resilience brake of each finger were disabled. This was similar to the concept of the current methods, which only rendered shape and multilevel continuous resistive force feedback but did not provide rotational resistive force feedback or continuous resistive force feedback without resilience, as mentioned prior. For (E), the ELAXO device rendered multilevel continuous resistive force and rotational resistive force with or without resilience. Therefore, by comparing (R) and (E), we could observe whether the versatile feedback from ELAXO enhanced the VR experiences.

After the experimenter introduced the procedure of the study and calibrated the device, the participants could freely explore the VR scene. They were asked to experience all tasks but there was no certain order for them to experience the feedback from the tasks. The methods were counterbalanced. After the experiment, they were asked to fill out a questionnaire with a 7-point Likert scale, allowing decimal scores. They were interviewed for some feedback. The study took about one and a half hours.

5.3 Results and Discussion

The results are shown in Figure 11. A Friedman test and Wilcoxon signed-rank tests with Bonferroni correction for post-hoc pairwise tests were used for the analyses. Significant main effects are revealed in realism ($\chi^2(2) = 15.95, p < 0.001$) and preference ($\chi^2(2) = 7.45, p = 0.02$), but no significant main effect is found in distinguishability ($\chi^2(2) = 0.78, p = 0.68$) and enjoyment ($\chi^2(2) = 5.19, p = 0.08$). The post-hoc Wilcoxon pairwise tests show that in realism and preference, (E) significantly outperforms (V) and (R) but no statistical significance is between (V) and (R). Furthermore, although no significant main effect is found in Friedman test, the post-hoc pairwise tests show that (E) significantly outperforms (R) in enjoyment.

For resistive force feedback with resilience, 8 participants responded that they could feel that they were grasping elastic cubes, and the visual feedback matched the haptic feedback in (R) and (E). In this condition, the feedback from (R) and (E) were the same.

P4 mentioned the level 2 force feedback felt too strong for the large elastic cube, but P6 supposed that the two force levels from the cubes were quite similar. For (V), although most participants thought that the feedback from (V) was less realistic, 3 participants supposed that the feedback from (V) was acceptable, and P6 even preferred it due to the distinguishable vibration intensities.

For resistive force feedback without resilience, 7 participants mentioned that they could clearly perceive the resistive force when pressing the button and clamping the tenon and mortise joint, and felt no resilience when stopping moving the fingers inward or moving the fingers backward in (E). P8 commented that “*I did not feel any delay between rendering resistive force feedback and stopping rendering resilience force feedback.*” This shows that our resilience brake design in ELAXO effectively and smoothly renders resistive force feedback without resilience. For (R), P1, P4, P5 and P12 commonly mentioned that they could perceive resilience but the button or tenon did not bounce back in VR, which felt strange and reduced the realism. P9 and P12 supposed that the feedback from (V) was more realistic since it felt like the friction feedback when pressing or clamping.

For rotational resistive force feedback with resilience, 7 participants stated that the feedback from (E) felt like turning real knobs and they could clearly distinguish the two rotational resistive force levels from the knobs. However, P2 and P8 mentioned that the rotational resistive force feedback was too strong in (E), which made them difficult to turn the knobs. Furthermore, although P1 thought the feedback from (E) was realistic, but sometimes s/he felt the fingers were pulled by the rings. This might be caused by the guiding rings from the ELAXO device after the ring direction adjustment. Although the guiding rings were used as fixed pulleys, they still increased the resistive force due to the friction. 11 participants thought that (E) were more realistic than (R) since the cone-shaped cases in (E) guided the ring detachment direction for the rotation gestures. P10 commented that “*The feedback from the resistive force device (R) and ELAXO (E) were different. The force direction from the resistive force device (R) did not match the VR tasks, which reduced the immersion.*” This shows the essential of the proper ring detachment direction guidance in (E). Interestingly, although 5 participants supposed that the feedback from (V) was not realistic, P1, P4 and P10 still preferred the feedback from (V) because they thought that some real knobs clicked when being turned. Therefore, vibrotactile feedback was quite similar to the clicks of the knobs. P1 and P5 both proposed that combining the feedback from (V) and (E) could further increase the realism.

For rotational resistive force feedback without resilience, 8 participants agreed that the feedback from (E) matched their experiences of tightening screws in the real world. The screws became tighter when they released the screwdrivers, moved back the fingers and twisted the screwdrivers repeatedly. However, P4 and P8 said that the feedback was not very obvious so they had to perceive it carefully when performing the tasks. For (R), P3, P4 and P12 commented that the feedback with resilience pulling back their fingers when tightening screws was quite strange, which reminded them that the feedback was generated by the elastic bands, and broke the immersion. Furthermore, P1 mentioned that the resistive force feedback from (R) and (E) pulling the fingers from the back was different from the resistive force applied from the front of the fingers, which

reduced the realism. This issue was also mentioned in [8]. Interestingly, *P3* and *P12* mentioned that although they needed to perform a pinch gesture to detach the rings in (R), the gesture was similar to grasping the screwdriver tightly before twisting it. For (V), 7 participants supposed that the vibrotactile feedback was not proper feedback for tightening screws.

Based on the results and comments, the study verified that the feedback from (E) was significantly more realistic than that from (V) and (R). Therefore, the proposed method rendering resistive force and rotational resistive force with or without resilience enhances the users' VR experience. Furthermore, for some conditions, e.g., turning a knob with clicks or clamping a tenon and mortise with friction, combining vibrotactile feedback with the resistive force feedback from ELAXO could further improve the realism.

6 LIMITATIONS AND FUTURE WORK

The size of our device is still bulky. Compared with current exoskeletons, a band track with a band motor for each finger increases the weight and size. Since the band motor is at the end of the track, it interferes with the user more due to a long lever. The length of the track determines the maximum extension distance of the band. Although for the with resilience mode, the band's extension distance is the finger's moving distance in grasping or twisting, for the without resilience mode, the extension distance represents the sum of the finger's movement generating resistive force. Therefore, a short track could limit the experiences in the without resilience mode. We suppose that a curved track or other types of springs or elastic bands could reduce the size of the track in the future. Furthermore, downsizing the tracks also improves the collision issue between the exoskeleton parts of the adjacent fingers. Regarding the other collision issue between the ring and its cone-shaped case during the detachment and attachment, a guiding track or smoother case design could further reduce the collision. Although the inertia and collision cause by size and weight might interfere with users, we suppose that the rendered feedback is much more obvious, so the users still can clearly perceive the feedback, especially with visual feedback in VR. Therefore, the realism of ELAXO in the VR study is significantly better than others.

In addition, the exo-braking sets sometimes are not locked firmly since the 3D-printed ratchets and pawls are eroded after a while. Since the exo-braking sets have to bear the force extorted by the fingers, hand and wrist, the erosion is severe. We believe that using other materials or metals to fabricate the ratchets and pawls could improve the problem. Similarly, to prevent the exoskeleton from bending when grasping or twisting, which interferes and cancels the effects of the feedback, the current 3D-printed exoskeleton is thick. Using more robust but light material, such as carbon fiber, could reduce the current size and weight (540g) close to the commercial products, e.g., Cybergrasp (450g) and Dexmo (300g), to further achieve practicality and reduce unwanted inertia and collision while maintain the robustness. Furthermore, the exoskeleton's boundaries in VR could be also considered to prevent collision. Always showing the exoskeleton in VR may reduce immersion, so we propose to use an exoskeleton boundary detection system similar to Oculus guardian and Vive chaperone systems to show the exoskeleton's boundaries only when it is about to collide with

the other hand or body to handle the collision issue in the future. For the studies, although our participants have various hand sizes, including only a few female participants is still a limitation. To render rotational resistive force, the ring direction adjustment is performed but only in a certain direction, so the user can not freely determine the direction to twist an elastic object. This may require additional force sensing resistor (FSR) sensors attached to the inside of each ring to determine the user's intention of the twisting direction. Furthermore, to render rotational resistive force, we provide 1DoF instead of 2DoF for the MCP joint on ELAXO. This limits the fingers' abduction and adduction movements, especially for the dexterous thumb, although high degrees of freedom are rendered on the exoskeleton of ELAXO. To achieve 2DoF for the MCP joint of the thumb or even all fingers, a more sophisticated exo-braking set design is required. Finally, even though the current ELAXO design is only for three often-used fingers, the current design for each finger is modularized. Therefore, we can further wear the exoskeleton to the other fingers if we could downsize the current design as mentioned above, especially for the small and short ring and pinky fingers.

7 CONCLUSION

We proposed a wearable exoskeleton device, ELAXO, to render multilevel continuous resistive force and continuous rotational resistive force with or without resilience for grasping and twisting, respectively. By combining the exoskeleton, several mechanical designs and elastic bands' physical properties, ELAXO integrates versatile resistive force feedback to not only enhance VR experiences but also deliver haptic sensation tips in VR training. Resistive force measurement was performed to show how ELAXO can render versatile resistive force with various spring constants. We conducted a JND study for the four conditions, and obtained JND results, separately. Based on the results, we further performed a VR study to verify that compared with the current methods, the feedback from ELAXO significantly enhances the users' VR experience.

ACKNOWLEDGMENTS

This research was supported in part by Delta Research, Ministry of Science and Technology of Taiwan (MOST 110-2221-E-004-006, 111-2420-H-004-003, 111-2221-E-004 -008 -MY3) and National Chengchi University.

REFERENCES

- [1] Alexander Achberger, Fabian Aust, Daniel Pohlndt, Kresimir Vidackovic, and Michael Sedlmair. 2021. STRIVE: String-Based Force Feedback for Automotive Engineering. In *The 34th Annual ACM Symposium on User Interface Software and Technology (Virtual Event, USA) (UIST '21)*. Association for Computing Machinery, New York, NY, USA, 841–853. <https://doi.org/10.1145/3472749.3474790>
- [2] Merwan Achibet, Adrien Girard, Anthony Talvas, Maud Marchal, and Anatole Lécuyer. 2015. Elastic-Arm Human-scale passive haptic feedback for augmenting interaction and perception in virtual environments. In *2015 IEEE Virtual Reality (VR)*. IEEE, 63–68.
- [3] Merwan Achibet, Benoît Le Gouis, Maud Marchal, Pierre-Alexandre Leziart, Ferran Argelaguet, Adrien Girard, Anatole Lécuyer, and Hiroyuki Kajimoto. 2017. FlexiFingers: Multi-finger interaction in VR combining passive haptics and pseudo-haptics. In *2017 IEEE Symposium on 3D User Interfaces (3DUI)*. IEEE, 103–106.
- [4] Hrvoje Benko, Christian Holz, Mike Sinclair, and Eyal Ofek. 2016. NormalTouch and TextureTouch: High-Fidelity 3D Haptic Shape Rendering on Handheld Virtual Reality Controllers. In *Proceedings of the 29th Annual Symposium on User Interface*

- Software and Technology* (Tokyo, Japan) (*UIST '16*). Association for Computing Machinery, New York, NY, USA, 717–728. <https://doi.org/10.1145/2984511.2984526>
- [5] Francesco Chinello, Monica Malvezzi, Claudio Pacchierotti, and Domenico Prattichizzo. 2015. Design and development of a 3RRS wearable fingertip cutaneous device. In *2015 IEEE International Conference on Advanced Intelligent Mechatronics (AIM)*. IEEE, 293–298.
- [6] Inrak Choi and Sean Follmer. 2016. Wolverine: A Wearable Haptic Interface for Grasping in VR. In *Proceedings of the 29th Annual Symposium on User Interface Software and Technology* (Tokyo, Japan) (*UIST '16 Adjunct*). Association for Computing Machinery, New York, NY, USA, 117–119. <https://doi.org/10.1145/2984751.2985725>
- [7] Inrak Choi, Eyal Ofek, Hrvoje Benko, Mike Sinclair, and Christian Holz. 2018. CLAW: A Multifunctional Handheld Haptic Controller for Grasping, Touching, and Triggering in Virtual Reality. In *Proceedings of the 2018 CHI Conference on Human Factors in Computing Systems* (Montreal QC, Canada) (*CHI '18*). Association for Computing Machinery, New York, NY, USA, 1–13. <https://doi.org/10.1145/3173574.3174228>
- [8] Cathy Fang, Yang Zhang, Matthew Dworman, and Chris Harrison. 2020. Wireality: Enabling Complex Tangible Geometries in Virtual Reality with Worn Multi-String Haptics. In *Proceedings of the 2020 CHI Conference on Human Factors in Computing Systems* (Honolulu, HI, USA) (*CHI '20*). Association for Computing Machinery, New York, NY, USA, 1–10. <https://doi.org/10.1145/3313831.3376470>
- [9] Sean Follmer, Daniel Leithinger, Alex Olwal, Akimitsu Hogge, and Hiroshi Ishii. 2013. InFORM: Dynamic Physical Affordances and Constraints through Shape and Object Actuation. In *Proceedings of the 26th Annual ACM Symposium on User Interface Software and Technology* (St. Andrews, Scotland, United Kingdom) (*UIST '13*). Association for Computing Machinery, New York, NY, USA, 417–426. <https://doi.org/10.1145/2501988.2502032>
- [10] Massimiliano Gabardi, Massimiliano Solazzi, Daniele Leonardi, and Antonio Frisoli. 2016. A new wearable fingertip haptic interface for the rendering of virtual shapes and surface features. In *2016 IEEE Haptics Symposium (HAPTICS)*. IEEE, 140–146.
- [11] Xiaochi Gu, Yifei Zhang, Weize Sun, Yuanzhe Bian, Dao Zhou, and Per Ola Kristensson. 2016. Dexmo: An Inexpensive and Lightweight Mechanical Exoskeleton for Motion Capture and Force Feedback in VR. In *Proceedings of the 2016 CHI Conference on Human Factors in Computing Systems* (San Jose, California, USA) (*CHI '16*). Association for Computing Machinery, New York, NY, USA, 1991–1995. <https://doi.org/10.1145/2858036.2858487>
- [12] Teng Han, Qian Han, Michelle Annett, Fraser Anderson, Da-Yuan Huang, and Xing-Dong Yang. 2017. Frictio: Passive Kinesthetic Force Feedback for Smart Ring Output. In *Proceedings of the 30th Annual ACM Symposium on User Interface Software and Technology* (Québec City, QC, Canada) (*UIST '17*). Association for Computing Machinery, New York, NY, USA, 131–142. <https://doi.org/10.1145/3126594.3126622>
- [13] Seongkook Heo, Christina Chung, Geehyuk Lee, and Daniel Wigdor. 2018. Thor's Hammer: An Ungrounded Force Feedback Device Utilizing Propeller-Induced Propulsive Force. In *Proceedings of the 2018 CHI Conference on Human Factors in Computing Systems* (Montreal QC, Canada) (*CHI '18*). Association for Computing Machinery, New York, NY, USA, 1–11. <https://doi.org/10.1145/3173574.3174099>
- [14] Seongkook Heo, Jaeyeon Lee, and Daniel Wigdor. 2019. PseudoBend: Producing Haptic Illusions of Stretching, Bending, and Twisting Using Grain Vibrations. In *Proceedings of the 32nd Annual ACM Symposium on User Interface Software and Technology* (New Orleans, LA, USA) (*UIST '19*). Association for Computing Machinery, New York, NY, USA, 803–813. <https://doi.org/10.1145/3332165.3347941>
- [15] Ronan Hincket, Velko Vechev, Herbert Shea, and Otmar Hilliges. 2018. DexTER: Wearable Haptic Feedback for Grasping in VR via a Thin Form-Factor Electrostatic Brake. In *Proceedings of the 31st Annual ACM Symposium on User Interface Software and Technology* (Berlin, Germany) (*UIST '18*). Association for Computing Machinery, New York, NY, USA, 901–912. <https://doi.org/10.1145/3242587.3242657>
- [16] Seungwoo Je, Myung Jin Kim, Woojin Lee, Byungjoo Lee, Xing-Dong Yang, Pedro Lopes, and Andrea Bianchi. 2019. Aero-plane: A Handheld Force-Feedback Device that Renders Weight Motion Illusion on a Virtual 2D Plane. In *Proceedings of the 32nd Annual ACM Symposium on User Interface Software and Technology*. 763–775.
- [17] Seungwoo Je, Hyunseung Lim, Kongpyung Moon, Shan-Yuan Teng, Jas Brooks, Pedro Lopes, and Andrea Bianchi. 2021. Elevate: A Walkable Pin-Array for Large Shape-Changing Terrains. In *Proceedings of the 2021 CHI Conference on Human Factors in Computing Systems* (Yokohama, Japan) (*CHI '21*). Association for Computing Machinery, New York, NY, USA, Article 127, 11 pages. <https://doi.org/10.1145/3411764.3445454>
- [18] Chi-Jung Lee, Hsin-Ruey Tsai, and Bing-Yu Chen. 2021. HairTouch: Providing Stiffness, Roughness and Surface Height Differences Using Reconfigurable Brush Hairs on a VR Controller. In *Proceedings of the 2021 CHI Conference on Human Factors in Computing Systems*. 1–13.
- [19] Jaeyeon Lee, Mike Sinclair, Mar Gonzalez-Franco, Eyal Ofek, and Christian Holz. 2019. TORC: A Virtual Reality Controller for In-Hand High-Dexterity Finger Interaction. In *Proceedings of the 2019 CHI Conference on Human Factors in Computing Systems* (Glasgow, Scotland UK) (*CHI '19*). Association for Computing Machinery, New York, NY, USA, 1–13. <https://doi.org/10.1145/3243584.3243606>
- [20] Pedro Lopes, Sijing You, Lung-Pan Cheng, Sebastian Marwecki, and Patrick Baudisch. 2017. Providing Haptics to Walls & Heavy Objects in Virtual Reality by Means of Electrical Muscle Stimulation. In *Proceedings of the 2017 CHI Conference on Human Factors in Computing Systems* (Denver, Colorado, USA) (*CHI '17*). Association for Computing Machinery, New York, NY, USA, 1471–1482. <https://doi.org/10.1145/3025453.3025600>
- [21] Ken Nakagaki, Artem Dementyev, Sean Follmer, Joseph A. Paradiso, and Hiroshi Ishii. 2016. ChainFORM: A Linear Integrated Modular Hardware System for Shape Changing Interfaces. In *Proceedings of the 29th Annual Symposium on User Interface Software and Technology* (Tokyo, Japan) (*UIST '16*). Association for Computing Machinery, New York, NY, USA, 87–96. <https://doi.org/10.1145/2984511.2985457>
- [22] Ken Nakagaki, Daniel Fitzgerald, Zhiyao (John) Ma, Luke Vink, Daniel Levine, and Hiroshi Ishii. 2019. InFORCE: Bi-Directional ‘Force’ Shape Display for Haptic Interaction. In *Proceedings of the Thirteenth International Conference on Tangible, Embedded, and Embodied Interaction* (Tempe, Arizona, USA) (*TEI '19*). Association for Computing Machinery, New York, NY, USA, 615–623. <https://doi.org/10.1145/3294109.3295621>
- [23] Ken Nakagaki, Sean Follmer, and Hiroshi Ishii. 2015. LineFORM: Actuated Curve Interfaces for Display, Interaction, and Constraint. In *Proceedings of the 28th Annual ACM Symposium on User Interface Software and Technology* (Charlotte, NC, USA) (*UIST '15*). Association for Computing Machinery, New York, NY, USA, 333–339. <https://doi.org/10.1145/2807442.2807452>
- [24] Romain Nith, Shan-Yuan Teng, Pengyu Li, Yujie Tao, and Pedro Lopes. 2021. DextrEMS: Increasing Dexterity in Electrical Muscle Stimulation by Combining It with Brakes. Association for Computing Machinery, New York, NY, USA, 414–430. <https://doi.org/10.1145/3472749.3474759>
- [25] Domenico Prattichizzo, Francesco Chinello, Claudio Pacchierotti, and Monica Malvezzi. 2013. Towards wearability in fingertip haptics: a 3-dof wearable device for cutaneous force feedback. *IEEE Transactions on Haptics* 6, 4 (2013), 506–516.
- [26] Neung Ryu, Hye-Young Jo, Michel Pahud, Mike Sinclair, and Andrea Bianchi. 2021. GamesBond: Bimanual Haptic Illusion of Physically Connected Objects for Immersive VR Using Grip Deformation. In *Proceedings of the 2021 CHI Conference on Human Factors in Computing Systems* (Yokohama, Japan) (*CHI '21*). Association for Computing Machinery, New York, NY, USA, Article 125, 10 pages. <https://doi.org/10.1145/3411764.3445727>
- [27] Samuel B. Schorr and Allison M. Okamura. 2017. Fingertip Tactile Devices for Virtual Object Manipulation and Exploration. In *Proceedings of the 2017 CHI Conference on Human Factors in Computing Systems* (Denver, Colorado, USA) (*CHI '17*). Association for Computing Machinery, New York, NY, USA, 3115–3119. <https://doi.org/10.1145/3025453.3025744>
- [28] Mike Sinclair, Eyal Ofek, Mar Gonzalez-Franco, and Christian Holz. 2019. CaptainCrunch: A Haptic VR Controller with User-Supplied Force Feedback. In *Proceedings of the 32nd Annual ACM Symposium on User Interface Software and Technology* (New Orleans, LA, USA) (*UIST '19*). Association for Computing Machinery, New York, NY, USA, 815–829. <https://doi.org/10.1145/3332165.3347891>
- [29] Alexa F. Siu, Eric J. Gonzalez, Shenli Yuan, Jason B. Ginsberg, and Sean Follmer. 2018. ShapeShift: 2D Spatial Manipulation and Self-Actuation of Tabletop Shape Displays for Tangible and Haptic Interaction. Association for Computing Machinery, New York, NY, USA, 1–13. <https://doi.org/10.1145/3173574.3173865>
- [30] Bukan Son and Jaeyoung Park. 2018. Haptic Feedback to the Palm and Fingers for Improved Tactile Perception of Large Objects. In *Proceedings of the 31st Annual ACM Symposium on User Interface Software and Technology* (Berlin, Germany) (*UIST '18*). Association for Computing Machinery, New York, NY, USA, 757–763. <https://doi.org/10.1145/3242587.3242656>
- [31] Evan Strasnick, Christian Holz, Eyal Ofek, Mike Sinclair, and Hrvoje Benko. 2018. Hapti Links: Bimanual Haptics for Virtual Reality Using Variable Stiffness Actuation. In *Proceedings of the 2018 CHI Conference on Human Factors in Computing Systems* (Montreal QC, Canada) (*CHI '18*). Association for Computing Machinery, New York, NY, USA, 1–12. <https://doi.org/10.1145/3173574.3174218>
- [32] Yuqian Sun, Shigeo Yoshida, Takuji Narumi, and Michitaka Hirose. 2019. PaCaPa: A Handheld VR Device for Rendering Size, Shape, and Stiffness of Virtual Objects in Tool-Based Interactions. In *Proceedings of the 2019 CHI Conference on Human Factors in Computing Systems* (Glasgow, Scotland UK) (*CHI '19*). Association for Computing Machinery, New York, NY, USA, 1–12. <https://doi.org/10.1145/3290605.3300682>
- [33] Ryo Suzuki, Eyal Ofek, Mike Sinclair, Daniel Leithinger, and Mar Gonzalez-Franco. 2021. HapticBots: Distributed Encountered-Type Haptics for VR with Multiple Shape-Changing Mobile Robots. Association for Computing Machinery, New York, NY, USA, 1269–1281. <https://doi.org/10.1145/3472749.3474821>
- [34] Yujie Tao, Shan-Yuan Teng, and Pedro Lopes. 2021. Altering Perceived Softness of Real Rigid Objects by Restricting Fingertip Deformation. In *The 34th Annual ACM Symposium on User Interface Software and Technology* (Virtual Event, USA) (*UIST '21*). Association for Computing Machinery, New York, NY, USA, 985–996. <https://doi.org/10.1145/3472749.3474800>
- [35] Shan-Yuan Teng, Tzu-Sheng Kuo, Chi Wang, Chi-huan Chiang, Da-Yuan Huang, Liwei Chan, and Bing-Yu Chen. 2018. PuPoP: Pop-up Prop for Virtual

- Reality. In *Proceedings of the 31st Annual ACM Symposium on User Interface Software and Technology* (Berlin, Germany) (*UIST '18*). Association for Computing Machinery, New York, NY, USA, 5–17. <https://doi.org/10.1145/3242587.3242628>
- [36] Hsin-Ruey Tsai, Yu-So Liao, and Chieh Tsai. 2022. ImpactVest: Rendering Spatio-Temporal Multilevel Impact Force Feedback on Body in VR. In *Proceedings of the 2022 CHI Conference on Human Factors in Computing Systems* (New Orleans, LA, USA) (*CHI '22*). Association for Computing Machinery, New York, NY, USA, Article 356, 11 pages. <https://doi.org/10.1145/3491102.3501971>
- [37] Hsin-Ruey Tsai and Jun Rekimoto. 2018. ElasticVR: Providing multi-level active and passive force feedback in virtual reality using elasticity. In *Extended Abstracts of the 2018 CHI Conference on Human Factors in Computing Systems*. 1–4.
- [38] Hsin-Ruey Tsai, Jun Rekimoto, and Bing-Yu Chen. 2019. ElasticVR: Providing Multilevel Continuously-Changing Resistive Force and Instant Impact Using Elasticity for VR. In *Proceedings of the 2019 CHI Conference on Human Factors in Computing Systems* (Glasgow, Scotland Uk) (*CHI '19*). Association for Computing Machinery, New York, NY, USA, 1–10. <https://doi.org/10.1145/3290605.3300450>
- [39] Hsin-Ruey Tsai, Chieh Tsai, Yu-So Liao, Yi-Ting Chiang, and Zhong-Yi Zhang. 2022. FingerX: Rendering Haptic Shapes of Virtual Objects Augmented by Real Objects Using Extendable and Withdrawable Supports on Fingers. In *Proceedings of the 2022 CHI Conference on Human Factors in Computing Systems* (New Orleans, LA, USA) (*CHI '22*). Association for Computing Machinery, New York, NY, USA, Article 430, 14 pages. <https://doi.org/10.1145/3491102.3517489>
- [40] Chih-An Tsao, Tzu-Chun Wu, Hsin-Ruey Tsai, Tzu-Yun Wei, Fang-Ying Liao, Sean Chapman, and Bing-Yu Chen. 2022. FrictShoes: Providing Multilevel Nonuniform Friction Feedback on Shoes in VR. *IEEE Transactions on Visualization & Computer Graphics* 01 (2022), 1–11.
- [41] Chi Wang, Da-Yuan Huang, Shuo-Wen Hsu, Cheng-Lung Lin, Yeu-Luen Chiu, Chu-En Hou, and Bing-Yu Chen. 2020. Gaiters: Exploring Skin Stretch Feedback on Legs for Enhancing Virtual Reality Experiences. Association for Computing Machinery, New York, NY, USA, 1–14. <https://doi.org/10.1145/3313831.3376865>
- [42] Yu-Wei Wang, Yu-Hsin Lin, Pin-Sung Ku, Yōko Miyatake, Yi-Hsuan Mao, Po Yu Chen, Chun-Miao Tseng, and Mike Y. Chen. 2021. JetController: High-Speed Un-grounded 3-DoF Force Feedback Controllers Using Air Propulsion Jets. Association for Computing Machinery, New York, NY, USA. <https://doi.org/10.1145/3411764.3445549>
- [43] Tzu-Yun Wei, Hsin-Ruey Tsai, Yu-So Liao, Chieh Tsai, Yi-Shan Chen, Chi Wang, and Bing-Yu Chen. 2020. ElastiLinks: Force Feedback between VR Controllers with Dynamic Points of Application of Force. In *Proceedings of the 33rd Annual ACM Symposium on User Interface Software and Technology* (Virtual Event, USA) (*UIST '20*). Association for Computing Machinery, New York, NY, USA, 1023–1034. <https://doi.org/10.1145/3379337.3415836>
- [44] Shigeo Yoshida, Yuqian Sun, and Hideaki Kuzuoka. 2020. PoCoPo: Handheld Pin-Based Shape Display for Haptic Rendering in Virtual Reality. In *Proceedings of the 2020 CHI Conference on Human Factors in Computing Systems* (Honolulu, HI, USA) (*CHI '20*). Association for Computing Machinery, New York, NY, USA, 1–13. <https://doi.org/10.1145/3313831.3376358>
- [45] André Zenner and Antonio Krüger. 2019. DragOn: A Virtual Reality Controller Providing Haptic Feedback Based on Drag and Weight Shift. In *Proceedings of the 2019 CHI Conference on Human Factors in Computing Systems* (Glasgow, Scotland Uk) (*CHI '19*). Association for Computing Machinery, New York, NY, USA, 1–12. <https://doi.org/10.1145/3290605.3300441>